Experimental study on single grit grinding of Inconel 718

Tahsin T Öpöz and Xun Chen

General Engineering Research Institute, Liverpool John Moores University, UK

Corresponding author:

Tahsin T Öpöz, General Engineering Research Institute, Liverpool John Moores University, Byrom Street, Liverpool L3 3AF, UK

Email: t.t.opoz@ljmu.ac.uk

Abstract

This paper presents an important investigation of material removal mechanism in grinding utilizing single grit scratch tests. The investigation helps people to understand the abrasive cutting behaviour when the abrasive cutting edge shape alters during single grit grinding. The results provide fundamental knowledge of the grinding material removal process which helps to improve grinding performance and quality. CBN grits of 40/50 mesh size were used to perform scratch tests on the alloy Inconel 718. The concepts of material pile up ratio and material removal strength were introduced to measure the material removal efficiency during grinding. It is found that pile up ratio decreases and material removal strength increases when the depth of cut increases, albeit the material removal mechanism is highly dependent on the abrasive grit cutting

edge shape. The material removal mechanism along the scratch length shows different behaviours at the entrance and exit sides of the scratching passes. When a grit was moving along its scratch path, it pushed material forward resulting in high material accumulation at the exit side of the scratches. Consequently, cutting is more prominent at the entrance side of the scratch, whereas ploughing or pile-up is extremely high at the exit side of the scratches. The research finding provides crucial information for grinding process optimization.

Keywords

Single grit grinding, material removal, ploughing, cutting

Introduction

High material removal rate and high surface quality are fundamental requirements of most grinding operations. The material removal ability of abrasive grits is of high interest in order to understand the grinding behaviour and its influence on the ground surface creation, particularly at the micro scale. With the entire grinding wheel-workpiece interaction [1, 2], it is difficult to evaluate an individual grit contribution to material removal and difficult to observe the effects of abrasive grit geometrical parameters, such as cutting edge shape, size, and depth of cut on the ground surface.

It was postulated that there could exist three stages of material removal in grinding, namely, rubbing, ploughing and cutting, to ultimately remove the material from the workpiece surface in the form of tiny chips [3]. As an abrasive grit slides on the workpiece surface for a small distance at the initial stage, the grit-workpiece interaction does not cause any permanent change on the surface topography, where the interaction only occurs in the elastic range and recovers due to elastic spring back effect after the interaction ends. This stage in the process is called rubbing. The ploughing stage is initiated with increasing penetration of the grit into the workpiece while the abrasive grit travels forward simultaneously. At this stage, the interaction occurs in both the elastic and plastic regions, but no real material removal occurs. When the shearing stresses increase beyond the tearing stresses, the ploughed material in front of the grit is finally removed from the workpiece in the form of chips. This stage is known as cutting. Among these stages, rubbing has negligible contribution to material removal, while ploughing plays a crucial role influencing energy consumption, surface roughness characterization, surface creation, and overall efficiency of the grinding process. In order to improve material removal efficiency, effective cutting should be maximized while rubbing and ploughing should be minimized because they consume energy without much contributing to the material removal [4].

To investigate single abrasive grit – workpiece interaction at the micro scale down to the submicron scale as well as the material removal characteristics at that range, single grit scratching tests have been utilized by many researchers[5-11]. Albeit, there are a substantial amount of tests performed by using a shaped abrasive grit or shaped cutting tool (known geometry) such as a diamond indenter or stylus [6, 12, 13], spherical tool [14], or negative rake cutter [15] to reduce shape factor influence during material removal, some experimental works also exist with the actual abrasive grits [5, 7, 8, 10, 16]. Shaped tools are good for experiments because they make easy comparisons with computational models[14, 17-22]. Besides, the shaped tools make parametric investigation easy to study the effect of speed, depth of cut, and hardness of materials on the material removal mechanisms by keeping the tool geometry stable. However, scratches with shaped tools diverge from the reality of actual grinding because the shapes of grit cutting edges continuously alter due to grit wear and fracture occurring during the grinding process. Takenaka [5] performed one of the earliest scratch tests and observed that a chip was produced even at a small depth of cut (lower than 0.5 μm) in the form of torn leaves from the workpiece surface although the rubbing and ploughing phases are also prominent in that range of depth cuts. Material removal was found mainly by the cutting process when the depth of cut is higher than 1 μm. Komanduri [23] investigated the grinding mechanism by using a highly negative rake angled diamond tool and observed chip formation up to a rake angle of -75º. Shaw [24] described the material removal

process during single grit-workpiece interaction as an extrusion-like mechanism. Wang et al [25] performed single grit scratching test with a conical diamond tool on pure titanium to characterize the material removal mechanism. The scratches depth of the tests was around 60 µm with a cutting speed of 0.54 m/s. They observed that there exists four zones in the interaction region, namely, a stagnant zone, a lamella zone with shear bands, a hardened sublayer zone, and a propagating zone during front ridge development in scratching test. Klecka and Subhash [26] investigated the material removal mechanism and associated damages in single and double scratches on alumina materials with different grain size (2 µm, 15 µm and 25 µm) using a diamond tip dresser as a scratch tool. Experimental result showed that there is a critical separation distance where the maximum material removal occurs for a pair of interacting scratches. Critical scratch separation distance was identified as 90 µm, 125 µm and 150 µm for the materials with grain size of 2 µm, 15 µm and 25 µm, respectively.

In the literature, the effect of cutting speed was studied mainly using shaped abrasive grits in order to minimize the influence of grit shape alteration during scratching test [11, 14, 27]. The majority of the research show that lower cutting speed and depth of cut increase the proportion of ploughing and make cutting less efficient[16, 27, 28]. The influence of cutting speed may not be captured appropriately when the grit feature changes significantly due to grit wear and fracture on the cutting edges. Thus, in this

research, the effect of cutting speed was not discussed due to significant alteration in the grit profile during scratching. Rather, this paper is mainly focused on morphological alteration in aspects of ploughing and cutting during scratching.

In this paper, the interaction between single abrasive grit and workpiece is studied in order to provide broader insight into the grinding mechanism. Although the influence of abrasive grit operating condition and the grit-workpiece interaction are the main issues to be investigated in this paper, the grit wear phenomenon, attritious wears, and fracture wear also exist on the cutting edges of the grit. Various wear phenomena on the grit can be observed by the variation of grit profiles in the scratch tests. For instance, the transformation of scratches from the single edge scratch to the multiple edge scratch can be considered as the result of the fracture of the grit during scratching test. Previous researchers [29] illustrated that attritious wear accounts for the wear flats on the grit cutting edges and cause a reduction in cutting ability of the abrasive grits, while fracture wear is part of abrasive grit loss due to grit breakage or entire abrasive grit dropping from the abrasive wheel due to bond fracture.

Experimental procedure

Scratching test setup

Single grit scratching tests were conducted on a Nanoform 250 Ultragrind machine centre. The machine centre is able to perform precision grinding and diamond turning with 3D complex surface forms and is capable of generating surfaces having an average surface roughness *Ra* better than 1 nm. In order to accommodate a single grit scratching test, a test setup was designed and manufactured as shown in Figure 1. The workpiece was mounted on a Kistler 3 axis piezoelectric force sensor. In addition, an acoustic emission (AE) sensor was mounted near the workpiece to detect the contact between the grit and the workpiece.

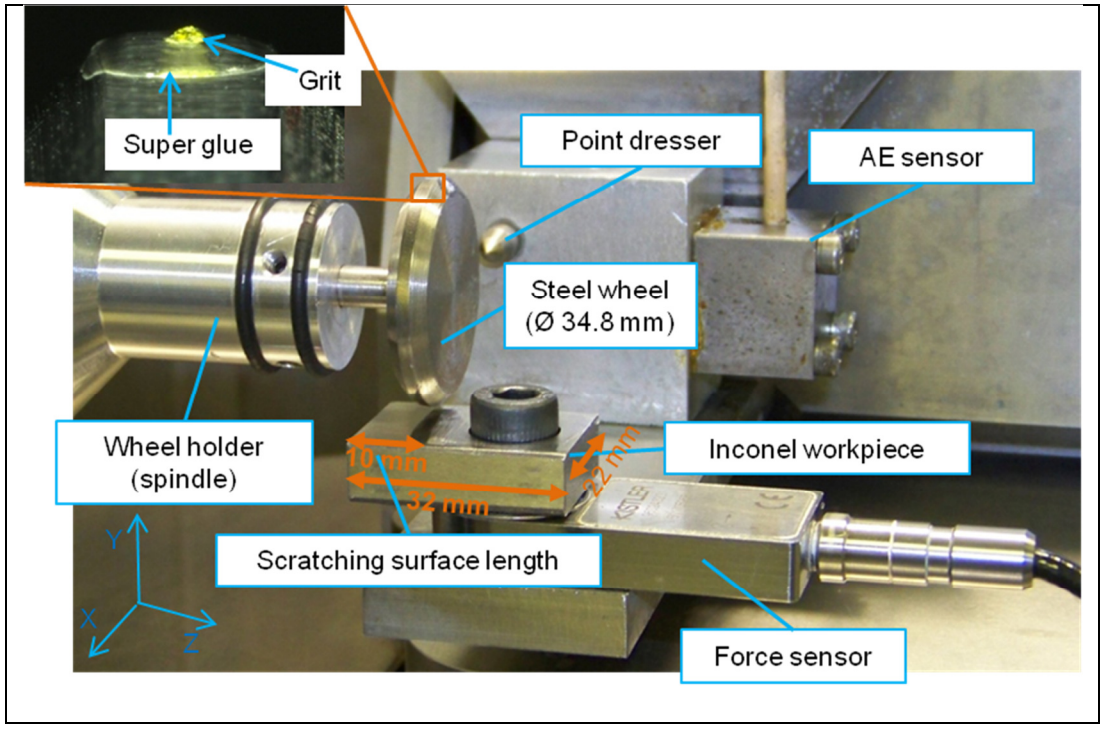

Figure 1. Single grit scratch test setup.

A Cubic Boron Nitride (CBN) grit of 40/50 mesh size was used for the scratching tests. Inconel 718 with a hardness of 355 HV at a 1 kg load was used as a workpiece. The workpiece surface was ground and polished prior to the scratching tests. The polished average surface roughness *Ra* was around 0.04 µm throughout the scratching surface. The diameter of the steel wheel was measured as 34.8 mm after grinding the circumferential surface of the steel wheel by using a high speed spindle (rotational speed N = 20000 rpm or peripheral speed V_c = 8.37 m/s). The steel wheel provided a run-out error less than 1 µm. A CBN grit was glued onto the circumferential surface of the steel wheel by using Loctite Super Glue as shown in Figure 1. The same grit was

used during the experiment as long as the grit stayed on the wheel surface. In case of the grit dropped off from the steel wheel, a new grit would be reinstalled to continue the experiment. Throughout this investigation, the same grit was used without experiencing the grit dropping off the steel wheel. A traverse scratching method was used to generate scratches at different depths of cut. Figure 2 shows the schematic of this traverse scratching method. The workpiece surface was tilted slightly to generate scratches leading to different depth of cuts; the height difference between the two ends of the scratching surface was less than 13 μm. More detailed description of the scratching process and the traverse scratching method were given in previous publication [7].

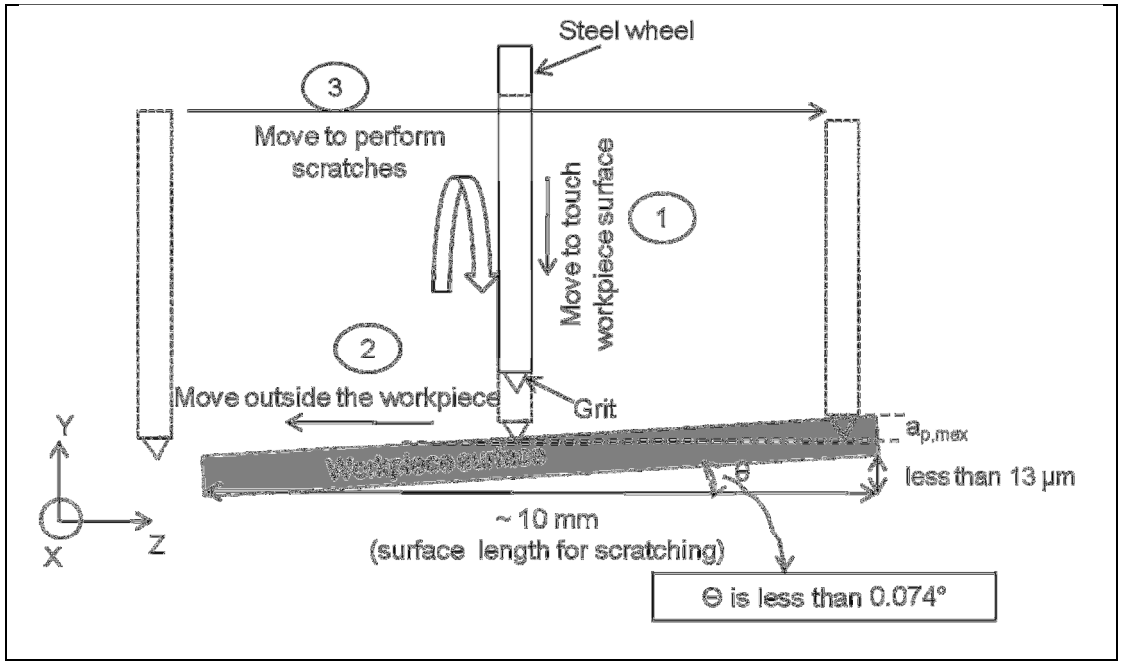

Figure 2. Scratching test methodology on a tilted surface ($a_{p,max}$: Maximum depth of cut).

Scratch profile measurement

A microscopic view of some single grit scratches on an Inconel workpiece with increasing depth of cut is shown in Figure 3. It can be seen that some scratches are less than 100 µm in length and less than 1µm in grove depth. The scratch profiles of the samples were measured by using a Talysurf CCI 3000 white light interferometer. A sample of the resulting 3D profile measurement is shown in Figure 4, where the gouging features can be clearly seen. After 3D profiles of the scratches were obtained, 2D profile sections were extracted from the deepest point of the scratches to measure

the groove depth, groove area, and pile-up area. Figure 5 shows the 2D profile of the scratches at the deepest point, from which the total pile-up and groove area sections will be used for analyses.

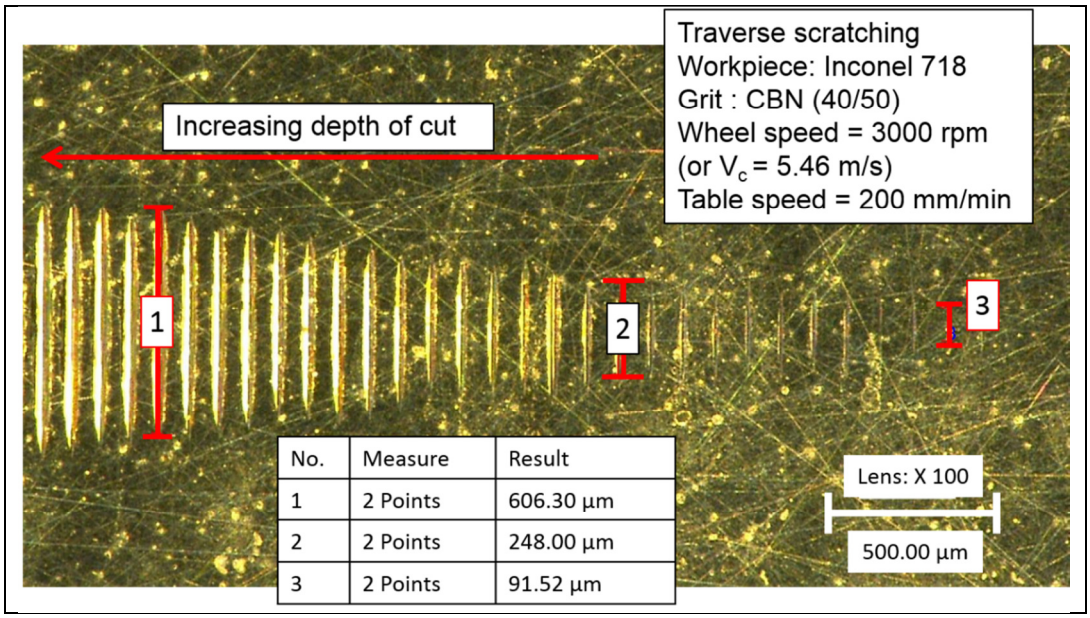

Figure 3. A view of scratches with increasing depths of cut.

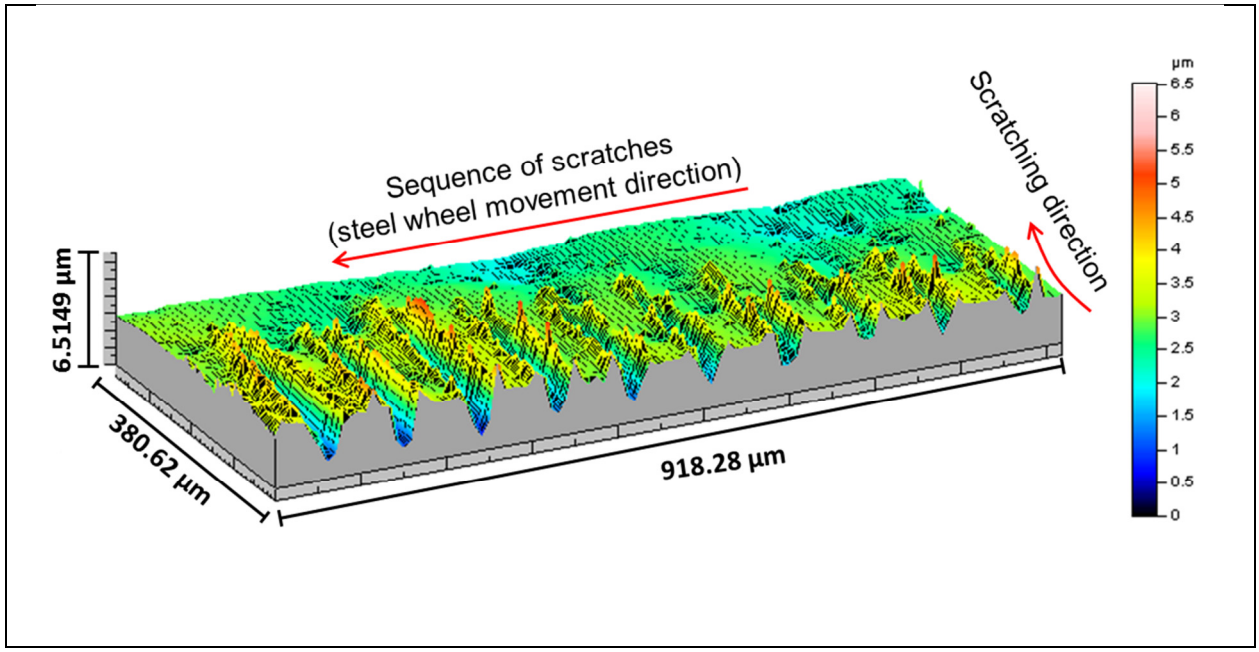

Figure 4. Example of 3D profile of scratches on the Inconel 718 workpiece (obtained from Figure 3).

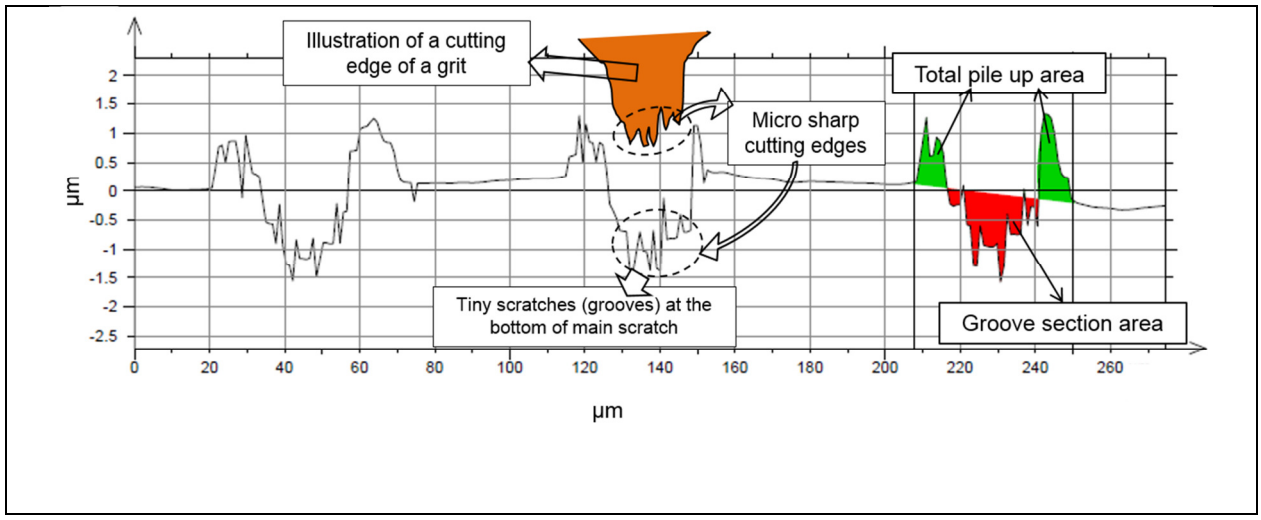

Figure 5. Scratch cross sectional profile, pile-up area and groove section area demonstration.

The profile of the scratches shows that the shape of the scratched grooves is altering at every consecutive scratch generation due to alteration of the cutting edge shape of the grit. With increasing numbers of scratch generation, the grit wear will present itself in the profile of the scratches. The alteration of the grit cutting edge occurs mainly due to wear flat generation and fracture of the grit. Ultimately, grit fracture leads to new cutting edges, which will maintain sharp cutting edges throughout the scratching. This phenomenon is also known as a self-sharpening during the grinding process [29]. Because it is impossible to measure the grit profile after each consecutive scratching pass under current test setup, the profile of the scratched grooves on the workpiece can be reasonably considered as the out-most profile of the grit, albeit errors may exist due to elastic deformation, which is insignificant [30, 31]. As seen in Figure 5, scratched grooves also included some tiny scratches (spikes) inside the main scratches. These tiny scratches could attribute to the existence of sharp cutting edges on the grit edge which engaged with the workpiece. Although these tiny scratches could also be generated due to brittle fracture of the workpiece material, repeated pattern of the cross section profiles observed in the consecutive scratches (Figure 5), however, suggest that the tiny scratches were generated mainly by micro sharp cutting edges existing on the grit surface. In some circumstances, the grit fracture could be very influential in creating

multiple cutting edges which would, therefore, generate multiple edge scratches. Figure 6 shows the point where the multiple edge scratches appeared on the Inconel 718 workpiece after production of several single cutting edge scratches. Similar phenomenon was also observed during the scratch tests on an EN24T steel where the adjacent multiple scratches developed after some single edge scratches' formation as shown in Figure 7 [32]. In the case of multiple cutting edges with different cutting edge heights, increasing the depth of cut could facilitate the generation of multiple edge scratches. It was observed that the single grit cutting edge can be altered into three different shapes as shown in Figure 8, depending on the wear mechanism on the grit surface: (1) a single cutting edge which generates a single scratch (Figure 8-(a), (2) adjacent multiple cutting edges which act as a single cutting edge and create a single scratch (Figure 8-(b)), and (3) multiple distinct cutting edges which act as a separate cutting edges and generate separate scratches (Figure 8-(c)). It is noted that the cutting edges profiles, illustrated in Figure 8, were not measured profiles; they were hypothesized from the resultant scratches' cross section profiles. During the adjacent multiple cutting edges' engagement with the workpiece , the ploughed material at the adjacent side edge was squeezed together, which reinforced the ploughing function and led to less actual material removal (i.e. less efficient in terms of cutting) during scratching. On the other hand, during the multiple distinct cutting edges' engagement, the separate scratches due to the separate cutting edges on the grit do not contribute to

each other's material removal, thus, dissimilar to the former one (Figure 8-(b)). The material removal is strongly dependent on the grit cutting edge shape and other factors (such as, grit cutting edge sharpness, bluntness, and depth of cut). The efficiency of the material removal in terms of cutting and ploughing processes will be analyzed through the paper by introducing a concept of pile up ratio and material removal strength in later section. Figure 9-(a) shows an interferometry measurement of distinct scratches generated by different cutting edges on the same grit and Figure 9-(b) shows 2D profiles of the scratches extracted from Figure 9-(a). The grit fracture wear is considered as the main responsible mechanism that changed the single edge scratches into multiple edge scratches.

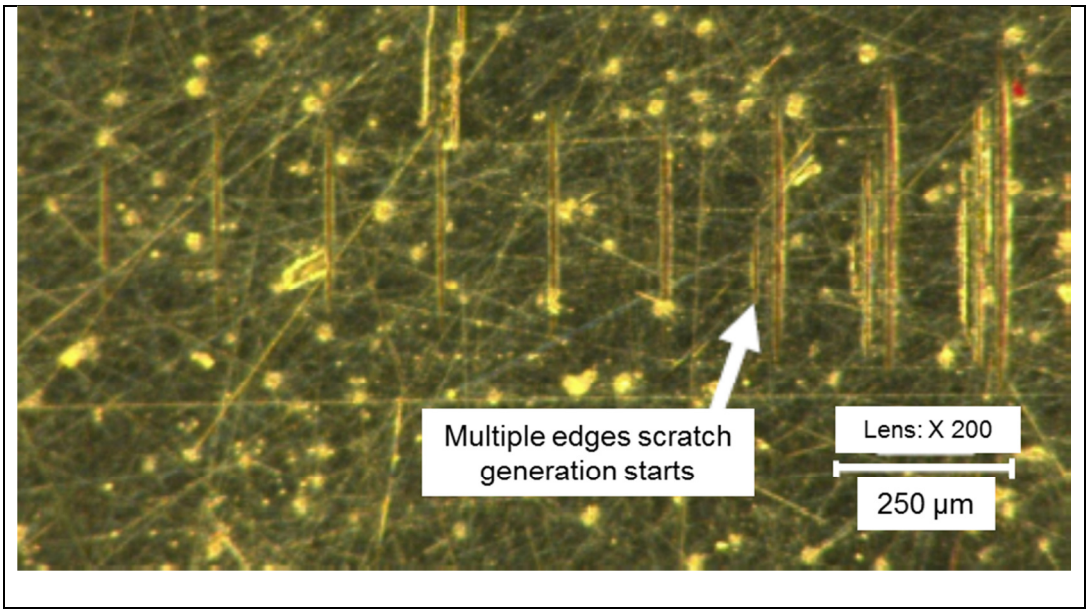

Figure 6 Microscopic picture shows that where the grit started to generate multiple edge scratches on the Inconel 718 workpiece.

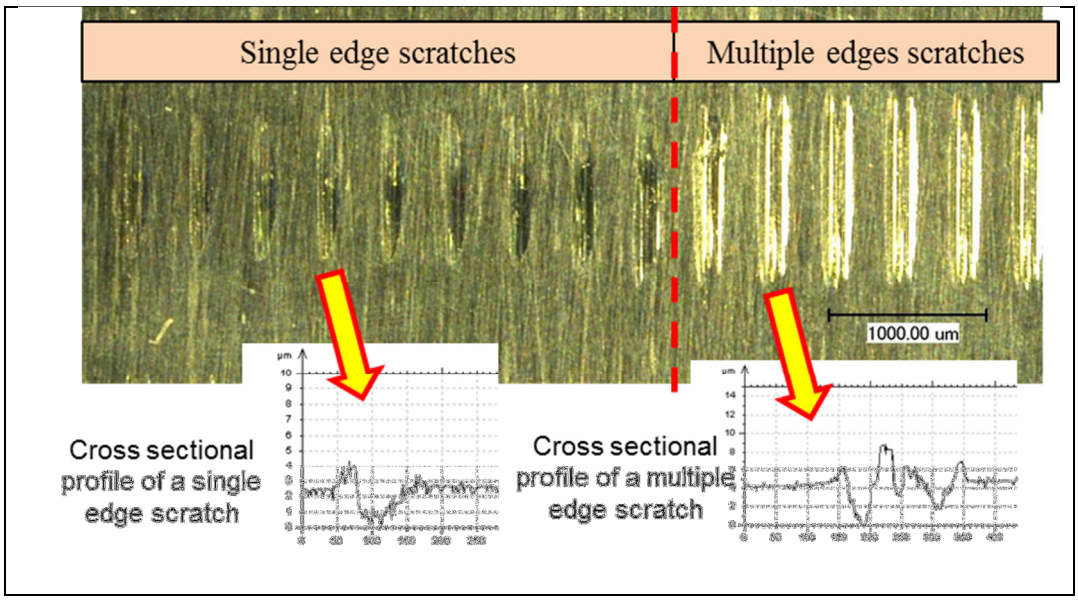

Figure 7 Transition from single edge scratches to multiple edge scratches on an EN24T steel workpiece [32] .

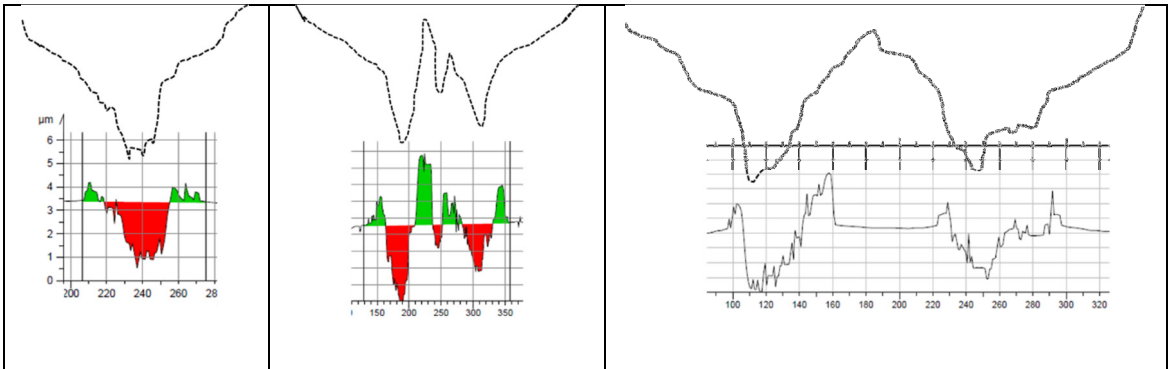

(a) Single cutting	(b) Adjacent multiple	(c) Multiple distinct cutting edges act as

edge creates a single edge scratch.	cutting edges act as a single cutting edge creates a single scratch with adjacent multiple grooves [7].	a separate cutting edge creates separate scratches.

Figure 8 Possible grit cutting edge profiles (not measured profile, it is a hypothesized profile from the cross section profile of the scratch) and alterations during sing grit scratching

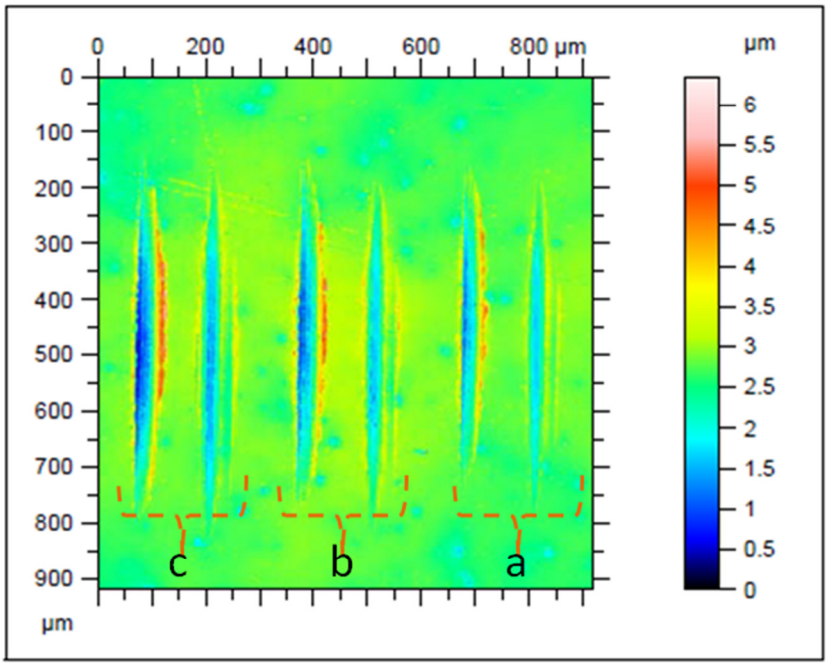

(a) 3D CCI interferometer measurement to show formation of separated scratches due to one pass of a grit

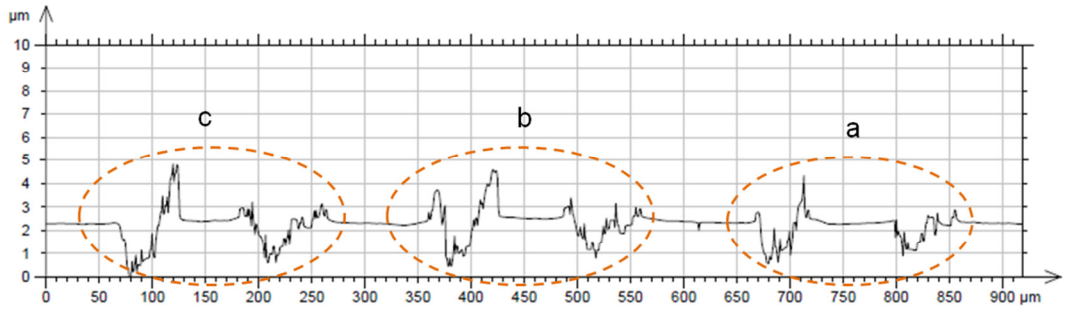

(b) 2D profile extraction from the middle of scratches which is shown in (a)

Figure 9. CCI Interferometer measurement for two separate scratches at every pass of grit.

In the scope of this work, the investigation of material removal mechanism during single grit scratching on the Inconel workpiece takes account of the grit cutting edge shape alteration in the ploughing and cutting mechanism analysis. Prominent material removal mechanism is decided using a measure of pile up ratio, which is defined as the ratio of total pile up area to total groove section area in the cross section under the consideration (Figure 10). The pile up areas and groove section areas were calculated at the deepest point of scratches by using Mountains software (TalyMap universal version 3.1.9), which is a software built for the surface measurement on Talysurf CCI 3000 interferometer. Accordingly, the material removal strength is defined as a new measure to quantify material removal efficiency along the scratch profile and it is determined by subtracting total pile up area from the groove cross section area as shown in Figure 10. According to the concept of pile up ratio and material removal strength, the higher the pile up ratio and material removal strength, the less the actual material removal, hence, the lower cutting efficiency. It is a simplified approach which does not take into account material flow (material accumulation) along scratching direction. Nevertheless, it is a good measure to demonstrate the influence of material removal across the cross sectional area of the scratch.

$$Material\ removal\ strength = GA - PA$$

$$Pile\ up\ ratio = PA / GA$$

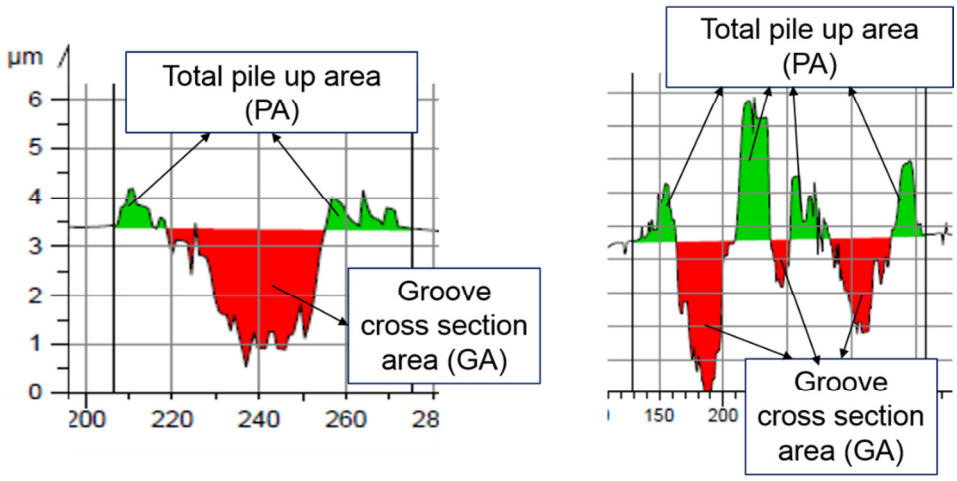

Figure 10 Material removal strength and pile up ratio with corresponding section profiles

Single grit grinding results and analyses

Material removal at the middle of scratching paths

The relations between the pile up ratio and the depth of cut or the groove cross section area at the middle of scratch paths were investigated by applying multiple scratches on Inconel 718 workpiece with various depths of cut ranged from around 0.5 μm to 6 μm. Figure 11 shows the pile-up ratio against depth of cut, where a steep decreasing trend of the pile up ratio with the increase of depth of cut presents when the depth of cut is less than 1.5 μm. When the depth of cut is greater than about 1.5 μm, the decreasing of the pile up ratio becomes less significant. The trend for the pile up ratio versus the groove cross section area shown in Figure 12 has similar features as that with the depth of cut.

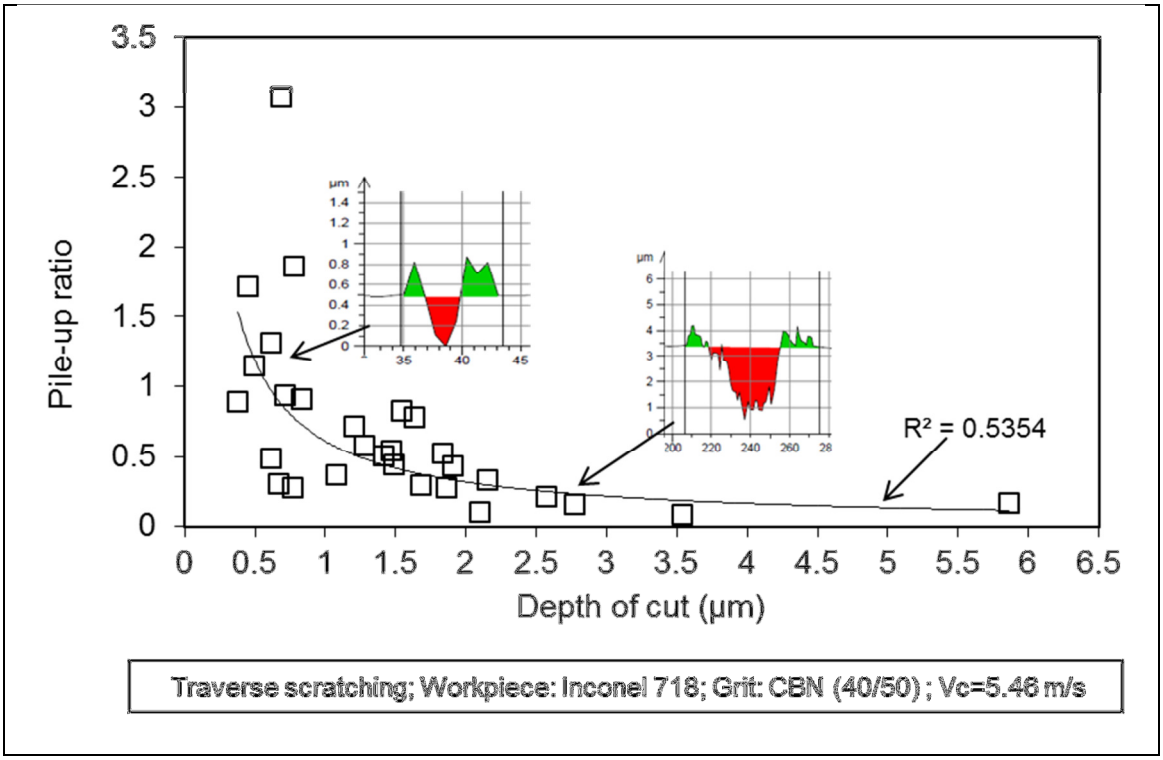

Figure 11. Pile-up ratio variation with depth of cut (obtained from Figure 4)

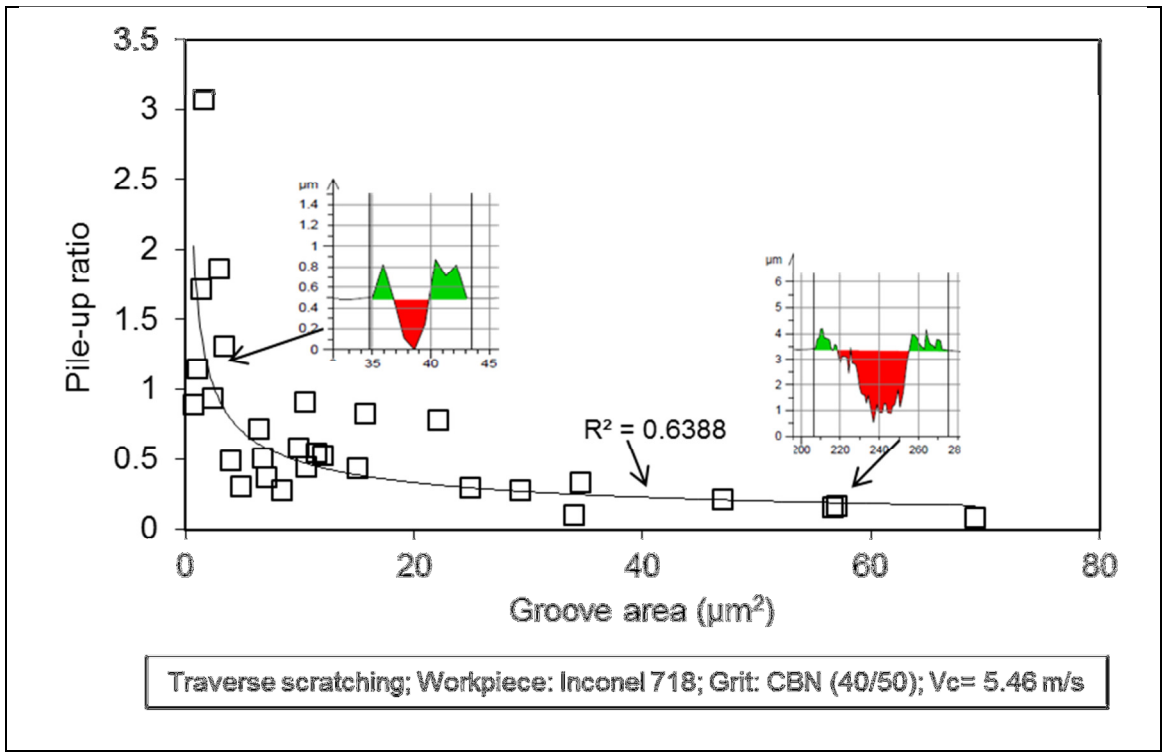

Figure 12. Pile-up ratio variation with groove area (obtained from Figure 4)

It should be pointed out that the pile up ratio can have a value larger than unity when the depth of cut is very small (e.g. < 1 μm) as shown in Figure 11, this can be attributed to ploughing action. It shows that less efficient cutting actions occur at small depth of cut, where material ploughing is more prominent. At small depths of cut, materials were deformed plastically and pushed forward creating ridges in both sides of the groove. Cutting might exist with a very small proportion compared to that exists at a higher depth of cut. When cutting action is not significant at small depths of cut, the pile up ratio becomes larger than unity. Hence, the larger pile-up ratio can be attributed to not only the smaller depth of cut makes the cutting inefficient but also the grit pushes materials forward leading to residual material accumulation at the different position along the scratch path.

As the definition of material removal strength was given in the previous section, the material removal strength could demonstrate the efficiency of material removal in relation to the cutting depth and the longitudinal position of a scratch. With the aid of material removal strength graph, a possible transitional point between material removal stages (ploughing and cutting) and their effects on contribution to the actual material removal can be identified. Figure 13 shows the variation of material removal strength with depth of cut using the same data set as in Figure 11. According to Figure 13, a transition point is obtained at around 1.5 μm depth of cut. The trend line of the material removal strength against depth of cut has a lower gradient than when the depth of cut is less than 1.5 μm. Up to the transition point the increase of the material removal strength could be attributed to the ploughing actions, but when the depth of cut is greater than 1.5 μm, the cutting actions become more prominent. Within the investigation range, the 1.5 μm depth of cut is a critical value to distinguish transition from the prominent ploughing mechanism to the prominent cutting mechanism. The negative values in Figure 13 represent the scratch section where the pile-up ratio is higher than 1 due to the material accumulation by ploughing actions as the grit advances. From the investigation, it was found that the identification of the transition point could be easier by using the material removal strength than using the pile up ratio because the pile-up ratio data were more scattered. However, it is not easy to obtain the

transition point for every set of measurements; the measured data set must include as wide a range of depths of cut as possible.

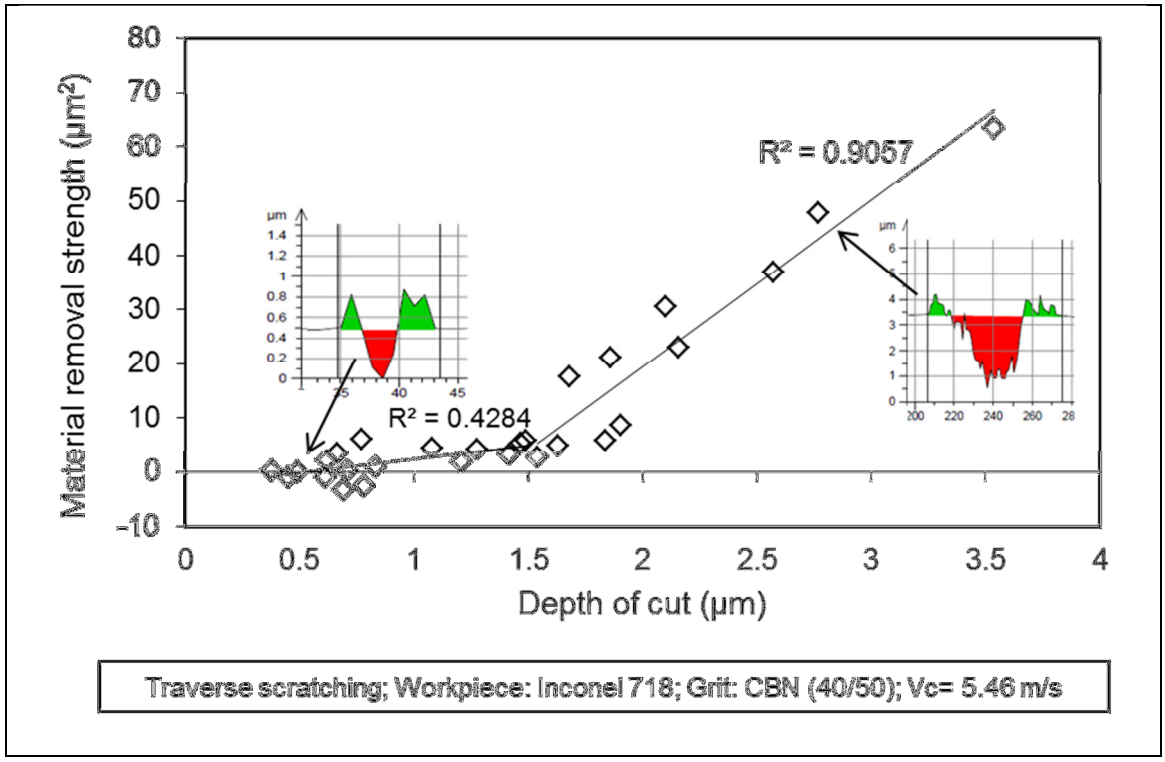

Figure 13. Material removal strength versus depth of cut (obtained from Figure 4).

Figure 14 and Figure 15 show the variation of the pile up ratio with depth of cut and groove area in a test when the grit has two distinct cutting edges interacting with the work sample at each pass of the grit and generates two distinct scratches with different profiles. The trend line looks generally similar to previous graphs for the single cutting edge grit, but the pile-up ratio looks to be highly scattered (lower coefficient of

determination R^2). Large variation in this test is due to the generation of two different scratches by two different cutting edges. The cross section profiles of different scratches given in Figure 14 can be considered as the reflection of the two different cutting edges' profiles. In Figure 14, at a depth of cut of about 1.5 μm it can be seen that the scratch profile above the trend line is sharper than the one below the trend line. The sharpness of the grit cutting edge was determined by examining the scratch cross section profile. Basically, scratch width to depth ratio and level of steepness of the cross section profile are the criteria for deciding a grit cutting edge is either sharp or less sharp. Thus, scratches are clustered into two groups according to their cross section profiles: scratches with sharp cutting edges and scratches with less sharp cutting edges. The former ones have higher pile up ratio, which are mainly placed above the trend line, compared to the later ones, which are placed below the trend line. However, some scratches generated with less sharp cutting edge are also placed above the trend line and result in high pile up ratio (e.g. with pile up ratio of 1.5 at 1.05 μm depth, seen on Figure 14). That means pile up ratio variation with depth of cut represents highly scattered distribution when two different scratch profiles are created due to multiple cutting edges on the grit. In that case, pile up ratio versus groove section area shows better correlation and also coefficient of determination R^2 value (0.4644) shows slightly better fit as shown in Figure 15. Majority of scratches with less sharp cutting edge have less pile up ratio placed below the scratches with sharp cutting edge have higher pile up

ratio. However, when the groove area is very small (e.g < 5 μm^2), pile up ratio could be very high for both less sharp and sharp cutting edges as shown in Figure 15. This suggests that cutting edges (sharp or less sharp) act similarly when creating very small scratches. Therefore, this different behaviour of cutting edges indicates that the sharp cutting edge could give higher pile-up ratio so the cutting efficiency could be lower when creating larger scratches with higher depth of cut.

Similarly, Figure 16 and Figure 17 show the variation of pile up ratio with depth of cut and groove area, respectively, for a different test. The scratches in this test also present two different scratch profiles created by two different cutting edges. Two cutting edges interact with the workpiece at each pass of the grit. One of the cutting edges was sharper while the other was less sharp. As shown in the right side of Figure 16 and Figure 17, the sharper cutting edge has a narrower width compared to the less sharp one. Thus, the sharper the grit cutting edge (narrower the width), the higher the pile-up ratio, while wider the cutting edges (less sharp) results in a lower pile-up ratio. This result is also consisting with previous graphs in Figure 14 and Figure 15.

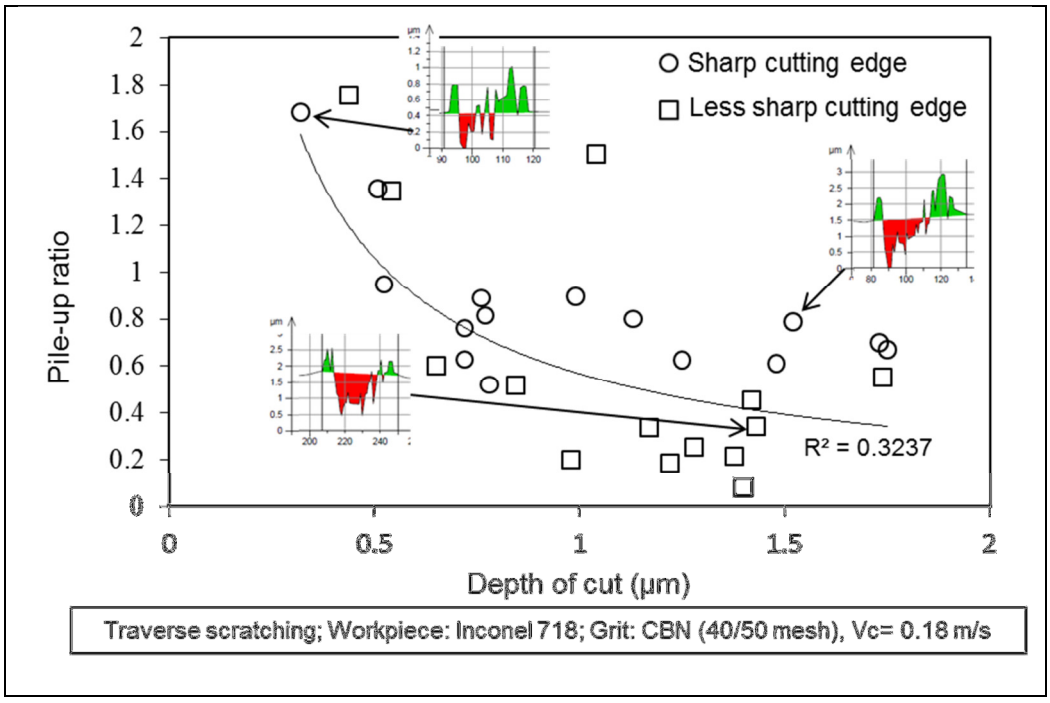

Figure 14. Pile-up ratio versus depth of cut (two separate scratches produced as a result of multiple distinct cutting edges on the grit).

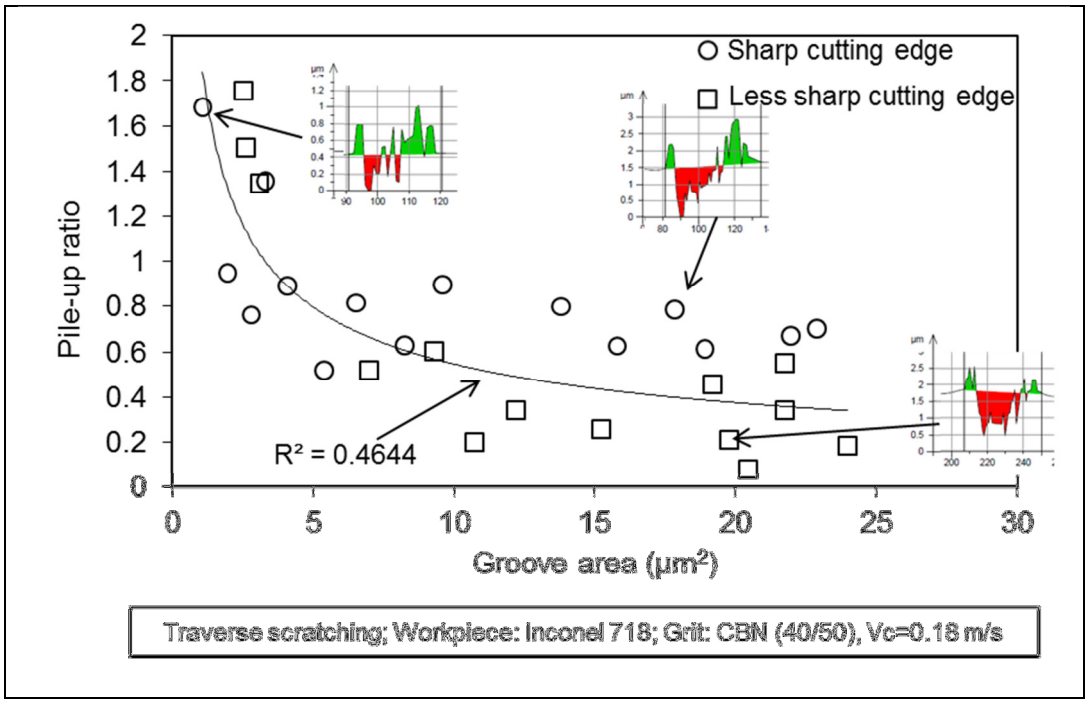

Figure 15. Pile-up ratio versus groove area (two separate scratches produced as a result of multiple distinct cutting edges on the grit).

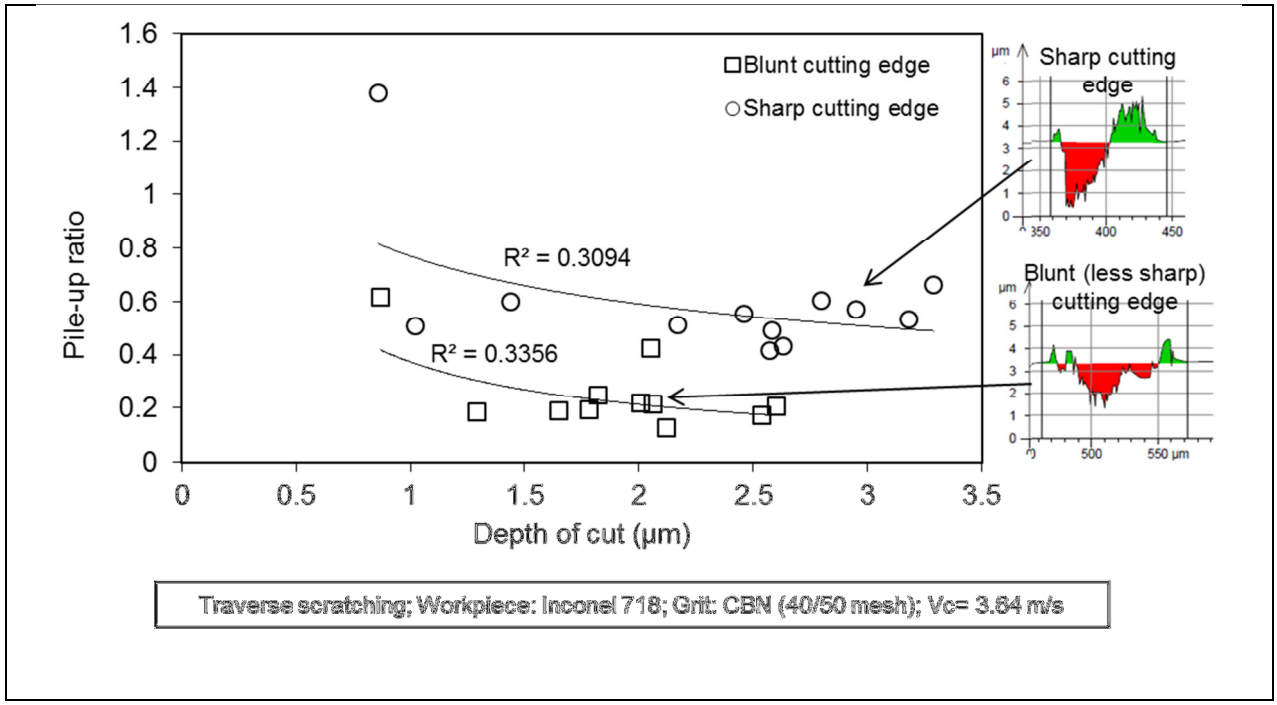

Figure 16. Pile-up ratio versus depth of cut (two separate scratches produced as a result of multiple distinct cutting edges on the grit, see Figure 9).

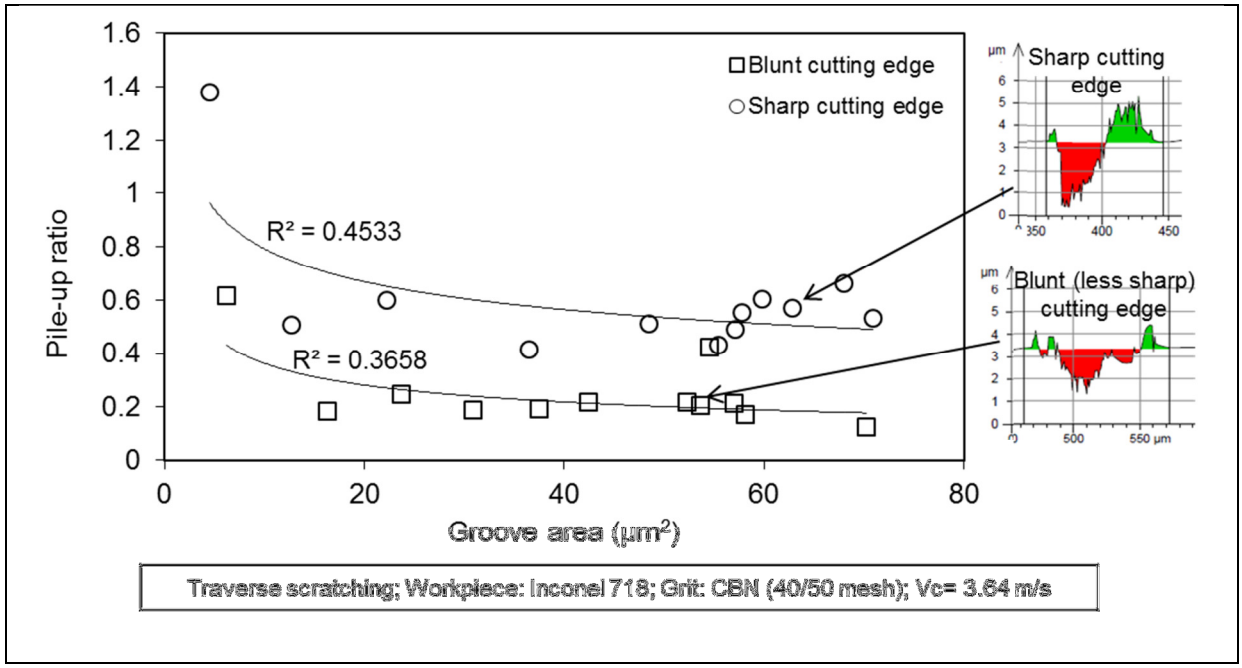

Figure 17. Pile-up ratio versus groove area (two separate scratches produced as a result of multiple distinct cutting edges on the grit, see Figure 9)

Material removal mechanism along scratch path

In the previous section, the measurements were done at the deepest point of the scratches. The material removal mechanism along a scratch path cannot be represented by a cross section obtained only at the deepest point of the scratch. A longitudinal and lateral cross-section along the scratch path on the Inconel 718 is as shown in Figure 18. The fundamental material removal characteristics along the scratch path were revealed.

Figure 19 shows the variation of the pile up ratio along the scratch path beginning from the initial grit-workpiece interaction and continuing to the end of scratch. The pile-up ratio is relatively smaller in the first half of the scratch than that obtained in the second half of the scratch as shown in Figure 19. At the initial stage of scratch in Figure 19, few spikes points for the pile up ratio represent material removal mechanism dominantly exist as a material swelling up without notable cutting because of very shallow cutting depth in that region (see Figure 20 for pile up ratio - depth of cut variation). Once remarkable cutting action began, pile up ratio dropped down to around 0.5, after than it is continuously rising with fluctuating trend towards the end of scratch. The reason of increasing pile up ratio towards the end of scratch could be partly attributed to ploughed material accumulation in front of the grit while the grit moves toward the end of scratch. At the end of the scratch, very high pile up ratios (~ 4 to 5) were measured with almost no cutting action. Grit pushed forward material towards the end of the scratch and material accumulation became very high at the exit side of the scratch. In that region, scratched groove by the grit is above the workpiece surface level, that is, the grit cut the accumulated material rather than work surface (see the end of scratch part in Figure 21). Similarly, little material swelling up above the surface level at the entrance of the scratch was observed (see the entrance of scratch part in Figure 21), but this cannot be attributed to material accumulation at this stage, it seems the grit squeezed some material up around two sides of it without cutting action when it started penetrating into

the workpiece. Interestingly, scratch depth profile along the scratch direction does not follow the ideal circular trajectory; it was observed uneven depth profile along the scratching direction as shown in Figure 21. This is because actual abrasive grit was used in the test rather than shaped cutting tool. Micro break and wear could take place on the grit cutting edges during single scratch generation, and this would change the cutting edge geometry. Sudden change in the cutting edge geometry resulted in uneven scratch depth profile. It can also be claimed that the cutting ability of the grit is better at the entrance side of the scratch than that at the exit side of the scratch. Material removal strength with depth of cut along the scratch path was graphed in Figure 22. It shows that cutting action is a significant material removal mechanism when increasing depth of cut. Negative values of material removal strength which are placed mainly at the exit side of the scratch represent the pile up ratio is above unity. The scratched groove in this region placed above the work surface level and formed in the accumulated material.

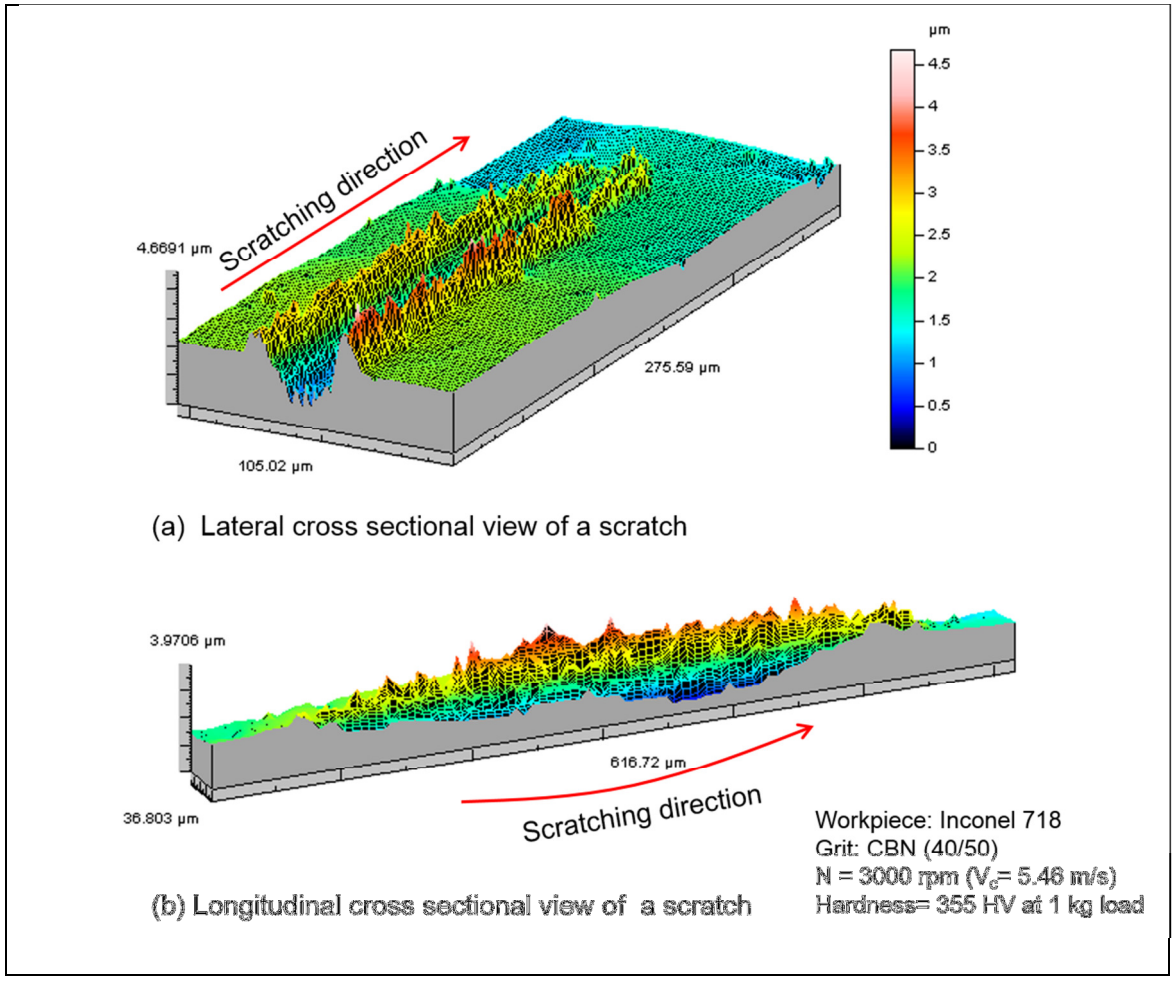

Figure 18. 3D view of single scratch (a) lateral cross-section, (b) longitudinal cross-section.

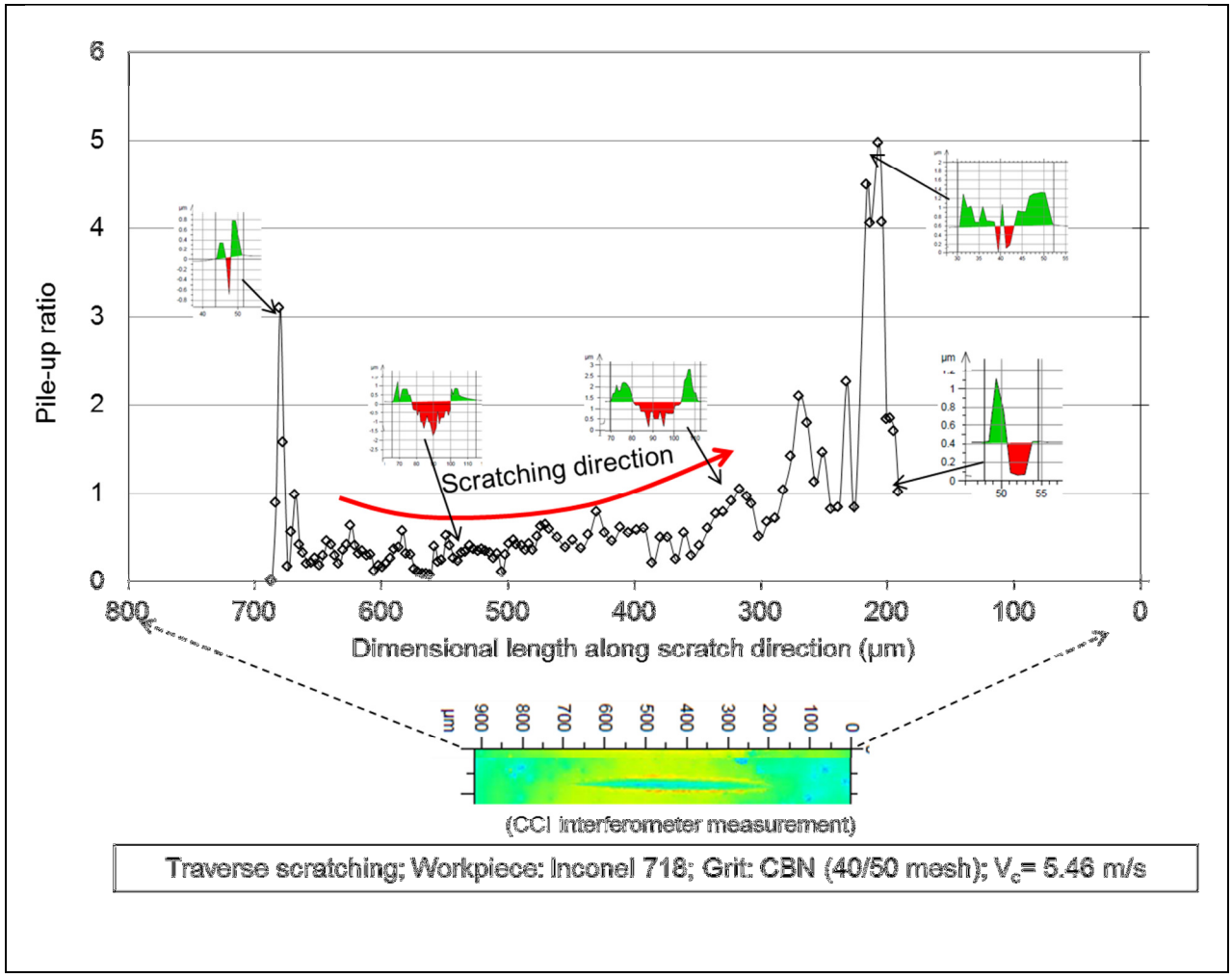

Figure 19. Variation of pile-up ratio along scratch path.

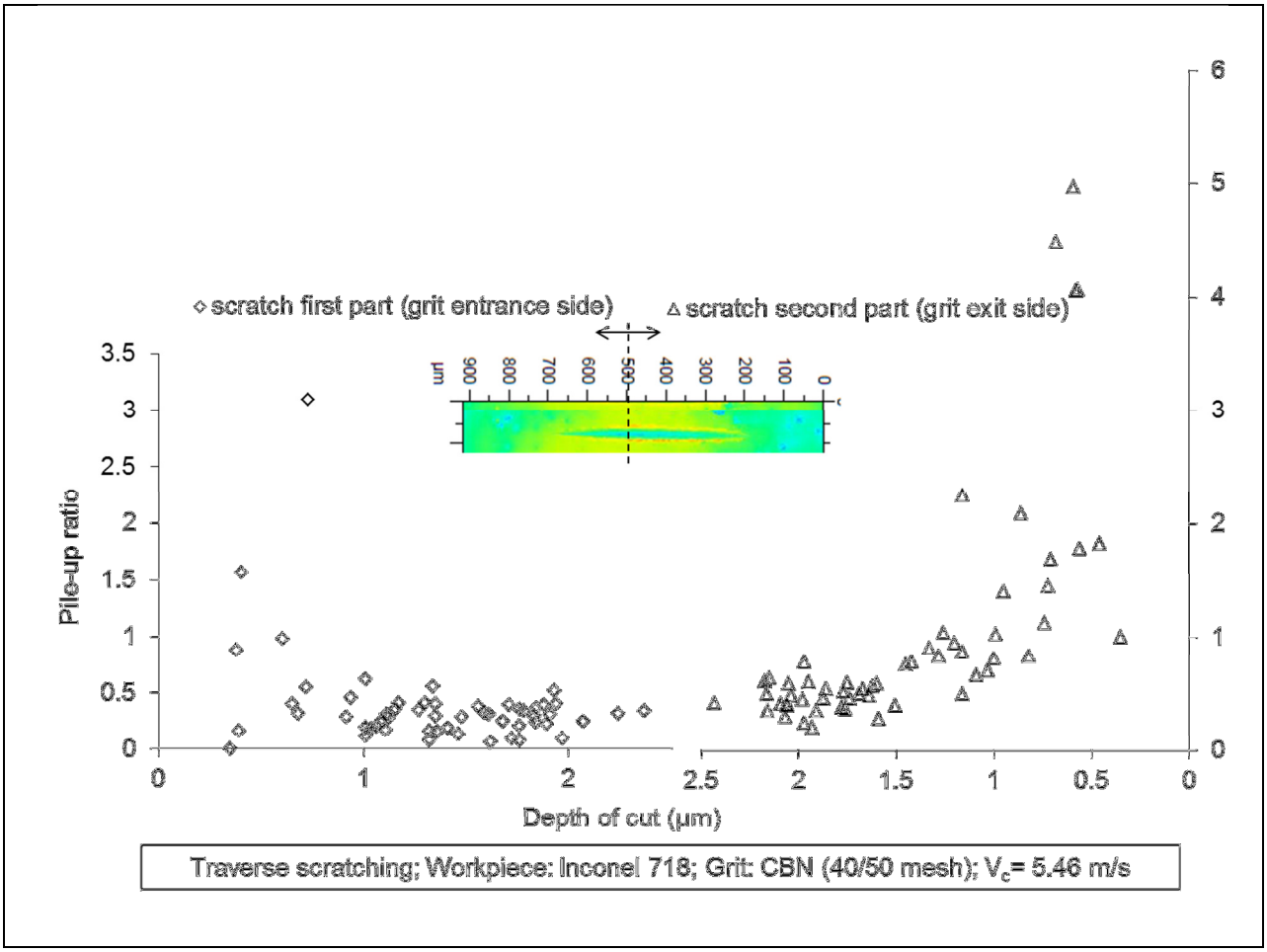

Figure 20. Pile-up ratio versus depth of cut along scratch length.

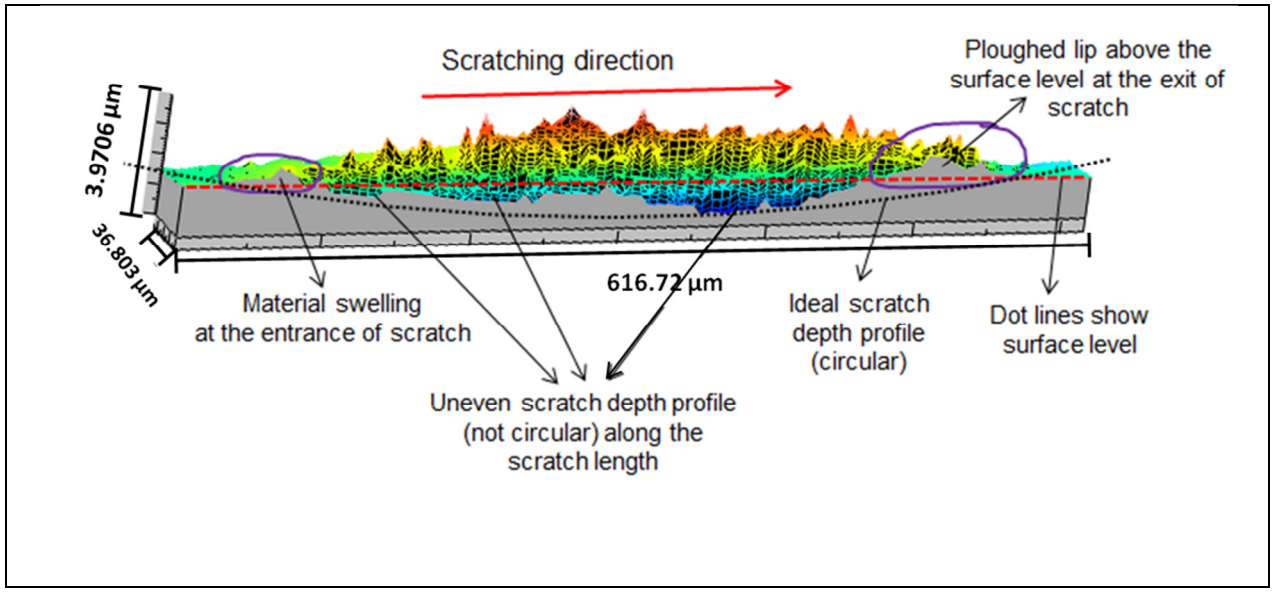

Figure 21. Longitudinal sectional view of a scratch with notations to show material removal characteristics along scratch path.

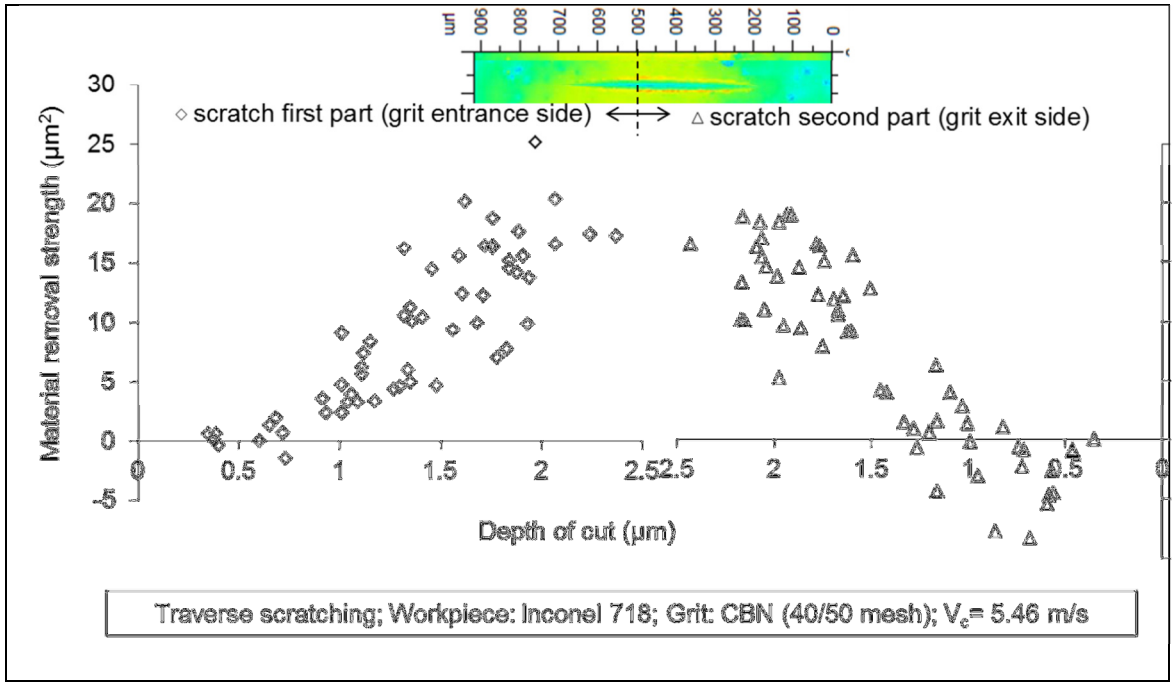

Figure 22. Material removal strength versus depth of cut along scratch path.

Summary

The cutting ability of a CBN grit on Inconel 718 material sample was studied by utilizing a series of single grit scratching tests. Similar to actual grinding processes, the abrasive grit cutting edge profile changed during the scratching tests. Experiments showed that the cutting edge shape alteration of the grit during scratching process was one of the most influential parameters to determine prominent material removal mechanism in terms of rubbing, ploughing and cutting. The pile up ratio and the

material removal strength were used as measures to represent the material removal mechanism. The scratches of single cutting edge and multiple cutting edges were generated, which demonstrated that different material removal mechanism could exist simultaneously in grinding due to various cutting edges presented. The pile up ratio decreases with increasing the depth of cut albeit it is highly dependent on the grit cutting edge shape. Sharp cutting edge resulted in higher pile up ratio compared to that found in less sharp cutting edge, when two distinct cutting edges exist on a grit. Besides, material removal strength increases with increasing depth of cut.

The material removal mechanism along the scratch path was also investigated in detail. It was found that the cutting ability of the grit was better at the entrance side of the scratch than that at the exit side of the scratch. Ploughed material due to material accumulation increases towards the end of scratch in the second half the scratch. Thus, pile up ratio was found dramatically high at the exit side of scratch compared to that found at the entrance side of the scratch. This phenomenon helps to explain the different grinding behaviour between up cut and down cut grinding.

References

1. Kannappan S and Malkin S. Effects of grain size and operating parameters on the mechanics of grinding. *Journal of Engineering for Industry - Transaction of the ASME*. 1972; 94: 833-42.

2. Zhong ZW and Venkatesh VC. Recent developments in grinding of advanced materials. *The International Journal of Advanced Manufacturing Technology*. 2009; 41: 468-80.
3. Hahn RS. On the nature of the grinding process. *Proceedings of the 3rd International Machine Tool Design & Research Conference*. Manchester1962, p. 129-54.
4. Ghosh S, Chattopadhyay AB and Paul S. Modelling of specific energy requirement during high-efficiency deep grinding. *International Journal of Machine Tools and Manufacture*. 2008; 48: 1242-53.
5. Takenaka N. A study on the grinding action by single grit. *Ann CIRP*. 1966; 13: 183-90.
6. Subhash G and Zhang W. Investigation of the overall friction coefficient in single-pass scratch test. *Wear*. 2002; 252: 123-34.
7. Öpöz TT and Chen X. Experimental investigation of material removal mechanism in single grit grinding. *International Journal of Machine Tools and Manufacture*. 2012; 63: 32-40.
8. Matsuo T, Toyoura S, Oshima E and Ohbuchi Y. Effect of grain shape on cutting force in superabrasive single-grit tests. *CIRP Annals-Manufacturing Technology*. 1989; 38: 323-6.
9. Ghosh S, Chattopadhyay AB and Paul S. Study of grinding mechanics by single grit grinding test. *International Journal of Precision Technology*. 2010; 1: 356-67.
10. Doyle ED. On the formation of a quick-stop chip during single grit grinding. *Wear*. 1973; 24: 249-53.
11. Anderson D, Warkentin A and Bauer R. Novel Experimental Method to Determine the Cutting Effectiveness of Grinding Grits. *Experimental mechanics*. 2011; 51: 1535-43.
12. Gu W, Yao Z and Liang X. Material removal of optical glass BK7 during single and double scratch tests. *Wear*. 2011; 270: 241-6.
13. Komanduri R, Varghese S and Chandrasekaran N. On the mechanism of material removal at the nanoscale by cutting. *Wear*. 2010; 269: 224-8.
14. Anderson D, Warkentin A and Bauer R. Experimental and numerical investigations of single abrasive-grain cutting. *International Journal of Machine Tools and Manufacture*. 2011; 51: 898-910.
15. Barge M, Rech J, Hamdi H and Bergheau JM. Experimental study of abrasive process. *Wear*. 2008; 264: 382-8.
16. Brinksmeler E and Glwerzew A. Chip formation mechanisms in grinding at low speeds. *CIRP Annals-Manufacturing Technology*. 2003; 52: 253-8.
17. Doman DA, Warkentin A and Bauer R. Finite element modeling approaches in grinding. *International Journal of Machine Tools and Manufacture*. 2009; 49: 109-16.

18. Doman DA, Bauer R and Warkentin A. Experimentally validated finite element model of the rubbing and ploughing phases in scratch tests. *Proceedings of the Institution of Mechanical Engineers, Part B: Journal of Engineering Manufacture*. 2009; 223: 1519-27.
19. Liang F, Qihong C, Kun S, Weiming L, Xiaofeng Z and Zhifu H. FEM computation of groove ridge and Monte Carlo simulation in two-body abrasive wear. *Wear*. 2005; 258: 265-74.
20. Öpöz TT and Chen X. Single Grit Grinding Simulation by Using Finite Element Analysis. *American Institute of Physics Conference Proceeding*. Paris: AIP, 2011, p. 1467-72.
21. Barge M, Kermouche G, Gilles P and Bergheau JM. Experimental and numerical study of the ploughing part of abrasive wear. *Wear*. 2003; 255: 30-7.
22. Kermouche G, Rech J, Hamdi H and Bergheau JM. On the residual stress field induced by a scratching round abrasive grain. *Wear*. 2010; 269: 86-92.
23. Komanduri R. Some aspects of machining with negative rake tools simulating grinding. *International journal of machine tool design and research*. 1971; 11: 223-33.
24. Shaw MC. *Principles of abrasive processing*. Clarendon Press Oxford, 1996.
25. Wang H, Subhash G and Chandra A. Characteristics of single-grit rotating scratch with a conical tool on pure titanium. *Wear*. 2001; 249: 566-81.
26. Klecka M and Subhash G. Grain size dependence of scratch-induced damage in alumina ceramics. *Wear*. 2008; 265: 612-9.
27. Patnaik Durgumahanti US, Singh V and Venkateswara Rao P. A new model for grinding force prediction and analysis. *International Journal of Machine Tools and Manufacture*. 2010; 50: 231-40.
28. Park HW, Liang SY and Chen R. Microgrinding force predictive modelling based on microscale single grain interaction analysis. *International Journal of Manufacturing Technology and Management*. 2007; 12: 25-38.
29. Chen X, Rowe WB, Mills B and Allanson D. Analysis and simulation of the grinding process. Part IV: Effects of wheel wear. *International Journal of Machine Tools and Manufacture*. 1998; 38: 41-9.
30. Öpöz TT and Chen X. An Investigation of the Rubbing and Ploughing in Single Grain Grinding using Finite Element Method. *8th International Conference on Manufacturing Research*. Durham , UK2010, p. 256-61.
31. Öpöz TT. Investigation of Material Removal Mechanism in Grinding: A Single Grit Approach. PhD thesis, The University of Huddersfield, September 2012.
32. Chen X and Öpöz TT. Comparison of materials removal characteristics in single and multiple cutting edge scratches. *Advanced Materials Research*. 2013; 797: 189-95.

Biographies

T. T. Öpöz is currently a senior lecturer in Liverpool John Moores University. He received his BSc degree in Mechanical Engineering from Gaziantep University, MSc degree in Mechatronics Engineering from Atilim University, PhD from Huddersfield University. He specialises in advanced manufacturing technologies including precision grinding, modelling and simulation of machining processes, and Electrical Discharge Machining.

X. Chen is currently a Professor of Manufacturing in Liverpool John Moores University. He has previously been an academic in the University of Huddersfield, the University of Nottingham, the University of Dundee and Fuzhou University and a royal research fellow in Liverpool Polytechnic. He specialises in advanced manufacturing technology including application of computing science, mechatronics and artificial intelligence to manufacturing process monitoring, control and optimisation, particularly to abrasive machining technology. He obtained his BEng from Fuzhou University, MSc from Zhejiang University and PhD from Liverpool John Moores University**.**